University of Baghdad
College of Engineering
JE
JOURNAL OF ENGINEERING

Journal of Engineering

journal homepage: www.jcoeng.edu.iq

Volume 32 Number 3 March 2026

Heat Dissipation Performance of High-Power CPUs using Finned Copper Foam Heat Sinks

Suha Shather Ismail, Wail Sami Sarsam*

Department of Mechanical Engineering, College of Engineering, University of Baghdad, Baghdad, Iraq

ABSTRACT

Thermal management has become a major issue in the latest high performance computing machines because high CPU temperatures result in inefficient performance and decreased hardware life span. In this work, the cooling performance of a finned metal foam heat sink (FMFHS) was examined. The pore density values of tested copper metal foam (CMF) samples with different values of PPI 5, 10 and 20, with a constant porosity of 90%. For reference, these samples were measured by a conventional Aluminum plate-fin heat sink (CHS). The work was performed under experimental conditions in which air directed over the heat sink surface at air velocities (2.5, 3.0 and 3.5 m/s). The environmental temperature was fixed at 27 °C. Findings indicated that pore density strongly affected on the cooling behavior. The 5-PPI foam showed an improved thermal performance better than CHS, due to the open pores and increased surface area, which enhance convective heat transfer. By contrast, the 10-PPI demonstrated moderate copper foam performance, placed between PPI 5 and CHS. The 20 PPI foam showed the lowest heat removal rates. Under these conditions, the 5 PPI design presented a 21.6 % increase in Nusselt number and a 16.9 % decrease in total thermal resistance at 3.5 m/s and 120 W compared to CHS. This confirms that using low PPI copper foams, such as 5-PPI in finned geometries, provides a considerable gain in cooling efficiency for high-power electronic components. Therefore, in high-power CPU cooling systems requiring high efficiency and compact size, it is recommended to use low PPI finned CMF heat sinks.

Keywords: Finned metal foam heat sink, Metal foam, Pore density, Forced convection, Thermal resistance.

1. INTRODUCTION

The ongoing evaluation of modern-day technology, the need for higher processing power in electronic devices has been continuously growing. In addition, constantly miniaturizing electronic components greatly increases heat generation in such a system. High thermal intensity impairs a device's efficiency, reliability, and lifespan, stressing the significance of

*Corresponding author
Peer review under the responsibility of University of Baghdad.
https://doi.org/10.31026/j.eng.2026.03.07

Article received: 22/11/2025
Article revised: 31/01/2026
Article accepted: 16/02/2026
Article published: 01/03/2026

the successful application of heat management in advanced electronics **(Güler et al., 2024; Moayad and Sarsam, 2025).**

An experimental investigation carried out by **(Nawaz et al., 2010)** using open-cell aluminum foam as a compact alternative to traditional brazed aluminum fin structures in heat exchangers. Their assessment employed a closed-loop wind tunnel setup to measure the characteristics of pressure drop and heat transfer, measured through. In doing so, the study emphasized how the importance of foam porosity above 0.90 and how metal foams improve heat transfer. Therefore, thermal management systems to be effective, flow control and refined design are essential**.** A numerical investigation of FMFHS subjected to uniform impinging airflow was conducted by **(Feng et al., 2015)**. Their study examined how changes in fin configuration, such as, including width, height, and length affected the heat transfer, and revealed that the finned metal foam system outperformed the conventional plate fin heat sink (CHS), achieving up to 26% higher heat transfer. However, this enhancement was accompanied by a significant increase in pressure drop. It also identified empirical relationships, which will pave the way for additional design optimization. **(Bayomy et al., 2016)** studied porous aluminium fins in comparison to CHS for Intel processors and found that aluminium foam pin fins outperformed solid copper pin fins regarding thermal performance. **(De Schampheleire et al., 2016)** conducted a combined experiment/ simulation to develop the thermal behavior of open-cell metal foams. To increase consistency in the results, they proposed a process that can closely monitor the foam structure with very fine features of the voxel profile. Their findings were different from their previous years' models; when they compared them to old models, they saw very evident differences and proposed improved CFD closure terms. These enhancements helped produce more accurate thermal predictions. **(Nima and Hajeej, 2016)** studied convective heat transfer using a horizontal fluid channel with aluminium metal foam blocks (100 × 50×10 mm) with PPI values between (10 - 30) under forced flow at Reynolds numbers between 500 and 2000. Their analysis revealed an improvement in heat transfer of up to 35 % relative to an unfilled channel. **(Shadlaghani et al., 2016)** studied the thermal effectiveness of the triangular fin design, both with and without longitudinal openings, and evaluated the resulting performance through graphical analysis by modifying the shape and dimensions of the fins with the fixed volume. The experimental results showed the correlation between the heat transfer rate in the triangular fins and the height-to-thickness ratio. It also showed that the thermal performance improvement was significantly higher with square and circular shape holes as compared with triangular holes. In their analysis, **(Andreozzi et al., 2017)** examined how different PPI configurations influence the thermal performance of impinging FMFHS when operated under the same pumping power conditions. Results presented 26% reduction in thermal resistance compared to the CHS and 2.5% decrease compared to fully optimized microchannel plate-fin heat sinks. **(Ali et al., 2018)** experimentally demonstrated that CMF with phase change materials (PCM) dramatically reduces thermal resistance compared to traditional heat sinks and therefore improves cooling efficiency. **(Welsford et al., 2018)** reported that high-porosity open-cell aluminum foams with a pore density of 10 PPI offer strong thermal efficiency and can serve as effective heat sinks for electronic applications such as CPU cooling. **(Hao and Zhang, 2019)** performed that the metal foam heat sink had a significantly superior thermal behavior, as it had a heat transfer coefficient that was 3.6 times higher than the finned heat sink, and all this without the heat building up, so it was more suitable for cooling CPUs with a continuously constant heat flux. **(Hoi et al., 2019)** examined how incorporating a fractal

insert into a fin-plate heat sink influences forced-convection heat transfer. Their findings showed that integrating the fractal network enhanced the heat sink's overall thermal performance under forced-flow conditions. **(Li et al., 2020)** performed a numerical investigation on a hybrid heat sink that combines metal foam with pin fins under local thermal non-equilibrium conditions. Their work showed that it improves the heat transfer by combination, and in this way contributes to the uniformity and a good temperature field. Impacted by porosity of the foam, pore density and the thermal contact resistance, researcher obtained that the contact resistance reduced the Nusselt number by almost 36%. This study observed that metal foam pin-fin material had suitable performance in all four domains with the thermal properties approximately 1.6 times thermal performance superiority compared to pin-fin heat sinks, demonstrating its potential for the advanced cooling applications pin-fin heat sinks. **(Qiu et al., 2020)** performed a porous copper micro-channel heat sink defined by high thermal conductivity and structural robustness. Results highlighted the importance of improving porosity and pore size, as these parameters significantly influence heat transfer performance and contribute to more energy-efficient CPU cooling. Numerical analysis was examined by **(Uglah and Jubear, 2020)** for natural convection in metal foam heat sinks designed with two fin profiles geometries curved and sharp edge. Results pointing to that rounding the fin edges enhanced the thermal performance, resulting in a 5.6% enhancement in the heat transfer coefficient and a 4 °C decrease in the base temperature compared with the sharp-edged fin design. **(Bianco et al., 2021)** performed the performance of finned and non-finned metal foam heat sinks on cooling and energy consumption. Results reveling that the capacity to successfully remove heat was significantly increased with fins, which resulted in a 3.3–3.5fold better heat removal than that of foam without fins at the same power. **(Li et al., 2021)** examined the MFPFHS design to improve electronic cooling under non-uniform heat flux conditions. Their configuration enhanced airflow distribution and increased the effective thermal conductivity of the heat sink. Under forced convection heat transfer. **(Singh et al., 2021)** studied the thermal performance of 25 different heat sinks including a micro-pin vanes square heat sink. Results showed that the micro-pin heat sink was the most efficient fin geometry. **(Kanate et al., 2022)** studied a numerical investigation on a conventional heat sink (CHS) for identifying the best fin pattern and simulated the airflow and heat transfer of extruded and cross-cut designs at a base temperature of 80°C with ambient air at 32°C, then compared the temperature drop, heat flux, and heat transfer coefficient. Their comparisons disclosed which geometry presented the best thermal performance. **(Liaw et al., 2022)** investigated a numerical study on hybrid heat sinks that utilize pin fins, metal foam, and a dielectric coolant during forced convection, conducted a single-step analysis using a copper foam with 10-PPI. For Reynolds number calculation from 100 to 1500 at a heat flux of 100 kW/m^2, measured various pin shapes, square, triangular, circular and also a configuration without pins. The triangular pins appeared best when foam was fully filled, whereas square pins were more effective in partially filled cases. In a general sense, the hybrid configuration achieved better for enhanced cooling for electronics applications. **(Ali and Ghashim, 2023)** conducted numerical analyses on forced convection in metal foam heat sinks and found that partial filling near the pipe wall with 10 PPI foam provided the best heat transfer enhancement with a Nusselt number ratio of 5.5 and better performance and more efficient thermal performance than 20 PPI and 40 PPI foams. **(Yudanto et al., 2023)** evaluated the performance of CPU heat sinks made from different materials, steel, aluminum, and copper, under various cooling orientations (horizontal, vertical, and mixed) and with multiple fan

configurations (2, 4, and 8 fans). Their experiments were carried out at an air velocity of 5 m/s for a 65 W CPU. **(Radmanesh et al., 2023)** performed numerical simulations of metal-foam heat sinks for air cooling of electronic devices, various foam porosities from 90 % to 60% was used, and founded that the optimal porosity was about 75 % corresponding to a geometry with good heat transfer as well as without an excessive loss. **(Mirshekar et al., 2023)** investigated the enhancement of cooling performance by partially filling a heat sink with a combination of metal foam and phase change material (PCM). Their experimental results showed that this approach improved both melting and solidification behavior, providing an effective balance between heat storage and thermal conduction. The metal foam increased the overall thermal conductivity, enabling faster heat transport through the PCM. **(Pires-Fonseca and Carrasco-Altemani, 2024)** provided a summary of the experimental and numerical research on CPU cooling with straight-fin and inline strip-fin heat sinks. These systems were tested at airflow speeds ranging (4-20 m/s), corresponding to Reynolds numbers between 810 and 3800. Despite the lower area of a strip-fin, its design results in better convective heat transfer and reduced thermal resistance. The numerical performance was well supported by experimental data. Their research showed the profound effect of fin geometry and flow condition on CPU temperature control.

(Haghighi et al., 2024) experimentally tested twelve heat sink designs (plate and pin-fin designs with rectangular, circular, and conical pins) under forced convection in fin counts of 5, 7, and 9, fin designs considering different air velocities. Using a 7-fin configuration has led to a 4–20% reduction of thermal resistance and a doubling of heat transfer coefficients compared to 5-fin and 9-fin configurations. Conical pin-fins with 7 or 9 fins facilitated convective heat transfer by up to 81% higher than plate fins, whereas 5-fin plate fins produced the least thermal resistance since they possessed a larger exposed surface area. **(Xiong et al., 2024)** studied heat transfer and flow behavior of open-cell copper foam of high porosity experimentally and numerically. In which cooling-induced porosity and airflow speed in the context of the porosity, as well as airflow speed and cooling performance comparison, then founded that higher air velocities significantly enhanced heat transfer, as did the internal porous structure, with a heavy impact on temperature distribution within the foam.

(Theeb and Hussain, 2024) described the integration of PCM with metal foams to further improve electronic cooling efficiency. The study demonstrated that the addition of metal foam to PCM materials increases their thermal conduction and assists in the melting and solidification processes faster. It also provided recent developments in the field of design enhancements and materials. It was determined that PCMs working in combination with metal foams can result in the improvement of temperature uniformity in electronic devices and an increase of heat absorbing ability. In particular, presented an overview of combining PCMs with metal foams to enhance electronic cooling efficiency. **(Wang et al., 2025)** investigated metal foam heat sinks with graded pore density to improve thermal performance under forced convection conditions. CFD simulations were used to examine eight composite foam geometries with variable pore density and constant porosity. The findings demonstrated that, in comparison to uniform foams, gradient pore structures have significantly lower flow resistance, particularly when high-porosity foam takes up a greater percentage of the channel. The best arrangement involved a negative pore gradient combining low and high PPI foams, supplying improved airflow characteristics and heat transfer efficiency. Copper foam heat sinks partially combined with phase change material (PCM) under forced air cooling were studied by **(Younus and Abedalh, 2025)**. A heated

copper plate was used to test various foam geometries and porosity levels under various airflow and power conditions. Results showed that hybrid foam–PCM arrangements significantly enhanced temperature control compared to conventional cooling systems. Higher porosity foam geometry and composite foam geometries achieved the best thermal performance. A review of heat sink for cooling laptop processors was given by **(Mangate et al., 2025)**. The thermal performance of several heat sink materials was studied and assessed in relation to compared copper and CHS heat sinks. Alternative materials were assessed based on their heat dissipation capability in electronic cooling applications. The research identified suitable material candidates that may replace CHS.

From the reviewed literature, it is evident that metal foam materials offer significant potential for enhancing heat dissipation in electronic cooling systems. However, most previous investigations have focused on aluminium foams or simple block-type geometries, with limited attention given to finned copper foams operating under forced convection and high thermal loads representative of CPU conditions. The influence of pore density on the thermal behavior of copper foam heat sinks has not been sufficiently addressed under identical airflow and heating conditions. Accordingly, this work sets out to perform experimental work to compare the heat dissipation behavior of finned copper foam heat sinks with 5, 10, and 20 PPI at different air velocities of 2.5, 3.0, and 3.5 m/s under a constant heat load of 120 W. The main objective is to find the most effective heat sink that will be able to obtain the least thermal resistance as well as the highest heat transfer efficiency when compared to CHS.

2. EXPERIMENTAL APPARATUS AND PROCEDURE

This section provides a detailed explanation of the main topics covered in this research, including the types of heat sinks employed, the experimental setup designed to evaluate their performance under forced convection, and the theoretical calculations based on the collected experimental results.

2.1 Heat Sinks Used in the Present Research

In this study, the CHS with dimensions of (100 × 100 × 20 mm) was used as the reference case to compare the performance of the proposed FMFHS. The CHS was made of aluminium alloy material featuring thermal conductivity of 167 W/m·K, and consisted of 16 straight fins with uniform geometry, and FMFHS configuration as shown in **Figs. 1 and 2**.

Fig. 3 represents the experimental apparatus schematically, and **Fig. 4**, photographically. The setup was designed to simulate a typical cooling configuration for a CPU model. It consisted of an electric heater and different heat sinks, i.e., CHS and FMFHSs. The FMFHS was tested using three pore density levels (PPI 5, 10, and 20) to examine the influence of foam structure on heat dissipation performance. The heater was powered through a 220-V supply and connected to a variable voltage transformer (Variac) to adjust the input power. A 220-V CPU fan was used to generate forced airflow over the heat sink, with air velocities of 2.5, 3.0, and 3.5 m/s controlled by a speed regulator. The air velocity inside the channel is not uniform, therefore, the velocity was measured at five different locations: four points near the channel walls and one point at the center, as shown in **Fig. 5**. The airflow was guided through an open-ended duct with a height of 250 mm to make sure uniform air distribution across the heat sink surface. In this experiment, a single heating power of 120 W was enforced to the heater to maintain steady heat input. The heater and fan were turned on simultaneously to initiate the heat transfer process.

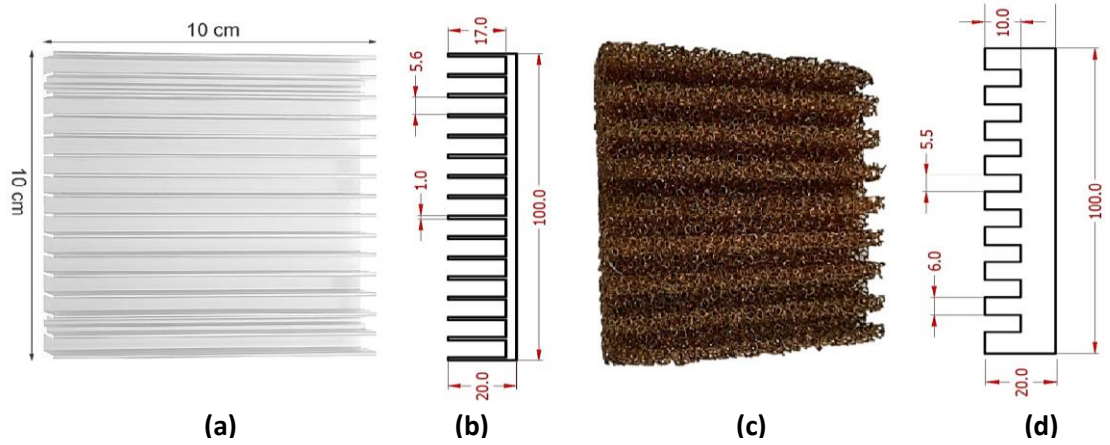

Figure 1. Picture and schematic geometry of (a & b) the CHS, and (c & d) the FMFHS used in the present work.

Figure 2. CMF with different PPI values of 5, 10, and 20 PPI before and after the cutting process.

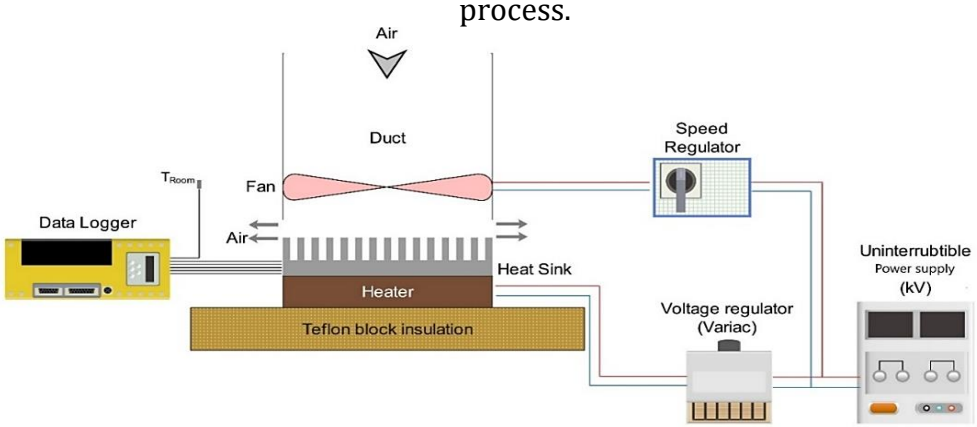

Figure 3. Schematic of the experimental system for forced convection heat transfer measurements

Temperature measurements were executed using six K-type thermocouples: five were joined to the base of the heat sink near the heated surface, and one was positioned to record the ambient air temperature, which was fixed directly into the heat sinks. The thermocouple junctions were inserted in to the base using small holes drilled at specific locations, ensuring tight contact with the metal surface and reduce measurement error. These locations included four points near the edges of the base and one point at the center, as shown in **Fig. 6**. This method provided precise monitoring of the heat sink temperature during operation and ensured reliable data for evaluating the thermal performance under different test conditions.

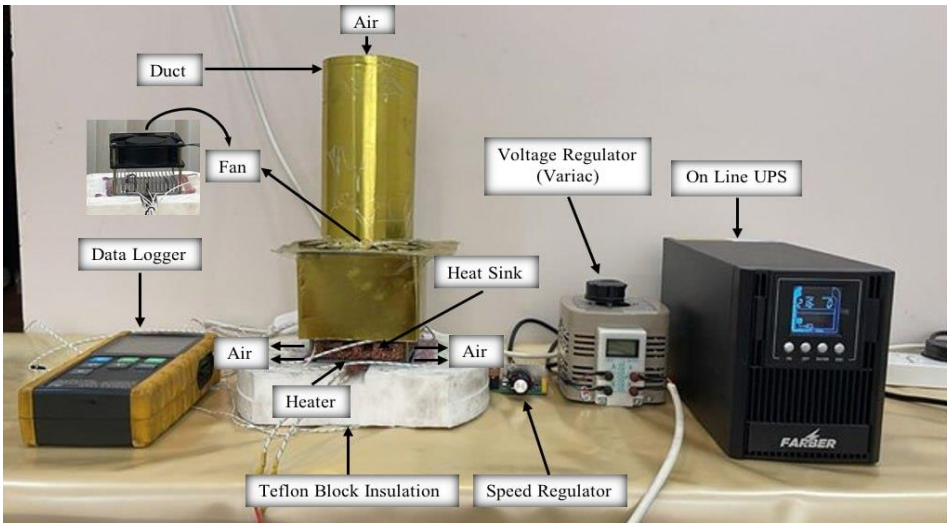

Figure 4. Photograph of the experimental apparatus.

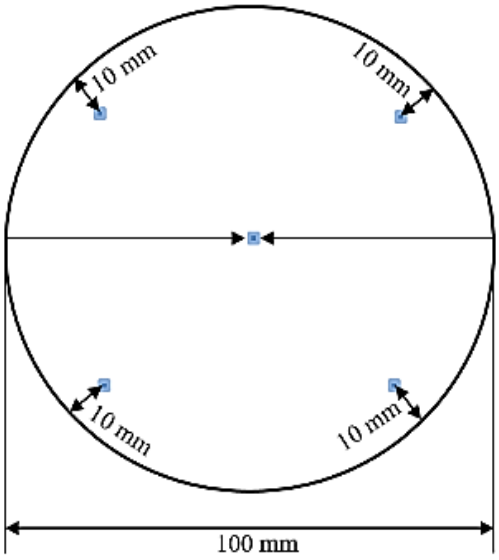

Figure 5. Measurement points used for air velocity calculation.

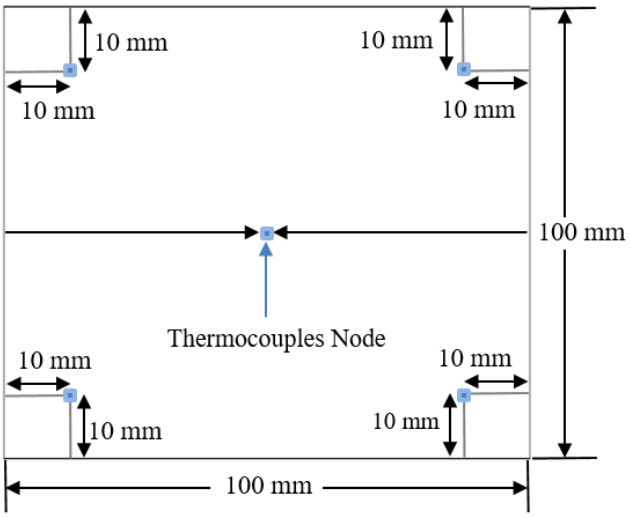

Figure 6. Distribution of Thermocouples on the base of heat sink.

2.2 Theoretical Calculations

The following quantities were calculated in the present work. The equivalent hydraulic diameter of the fin channel was expressed in Eq. (1) **(Adhikari et al., 2020)**:

$$D_h = 4\,A/P \tag{1}$$

Where:
$P = 2 \times (S + H)$: p is the wetted perimeter of the base heat sink.
$A = S \times H$: A is the cross–sectional area.
The heat transfer coefficient **(Heydari et al., 2020)** and Nusselt number **(Rashid et al., 2022)** were calculated as shown below:

$$h = Q/\,[A_b\,(T_b - T_a)] \tag{2}$$

h: Convective heat transfer coefficient
A_b: Base area of the heat sink
T_b: Base temperature of the heat sink
T_a: Ambient air temperature

$$Nu = (h\,D_h\,/\,K\,) \tag{3}$$

K: thermal conductivity of air

Where: the air properties were evaluated at the mean air temperature (T_f) **(Zografos et al., 1987)**

where,
$$T_f = (T_b + T_a)/2 \tag{4}$$
T_b: Base temperature of the heat sink

The power supplied to the heater comes from an electrical source. **(Mokhiamar et al., 2022)**

$$Po = V.I = Q \tag{5}$$

Po: electric heat input
V: Input voltage
I: Input current
Q: The heat transfer from the heated wall

Thermal resistance can be defined as follows **(Kim et al., 2003)**

$$R_{th} = \frac{(T_b - Ta\,)}{Q} \tag{6}$$

R_{th}: Thermal resistance
T_b: Base temperature of the heat sink

3. THERMOCOUPLE CALIBRATION

The thermocouples used in this experiment have been calibrated using three different liquids, as shown in **Fig. 7**. First, distilled water was used as a reference medium for measurement, and the calibration was performed at atmospheric pressure through measuring the ice temperature at 0 °C, and then boiling water at 100 °C. Subsequently, two different liquids, i.e., acetone and ethanol, were used to measure their boiling points at atmospheric pressure.

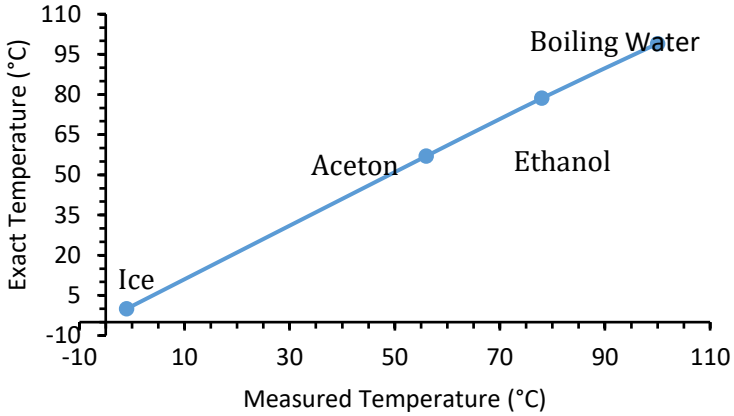

Figure 7. Thermocouple calibration curve.

4. UNCERTAINTY ANALYSIS

To make sure the experimental results are accurate, the uncertainties of the measuring instruments used in this study must be considered. All instruments were used according to the manufacturer's instructions to reduce errors and obtain reliable data. **Table 1** shows the main measuring devices and their related uncertainties.

Table 1. Measurement instruments and their corresponding uncertainties

Device	Type/Model No.	Measured Parameter	Uncertainty
Thermocouple	Type K	Base Temperature	±0.1°C
Data Logger	BTM-4208SD	Temperature	±0.8°C
Hot Wire Anemomete	YK-2005AH	Air Velocity	±5%
Clamp Meter	RMS MT-3202	ACV ACA	±0.8% ±1.2%
Uninterruptible power supply (UPS)	On-line UPS, 1 kVA–single phase	Input voltage regulator	±0.5%

The main sources of uncertainty in this experiment arise from errors in measuring power, thermocouple readings, and physical dimensions. The overall uncertainty of the parameters was determined through equation analysis suggested by **(Holman, 2012)**, and expressed as:

$$\delta R = \left(\frac{\partial R}{\partial x^1}\right)\delta x^1 + \left(\frac{\partial R}{\partial x^2}\right)\delta x^2 + \ldots + \left(\frac{\partial R}{\partial x}_n\right)\delta x \quad (7)$$

$$U_R = \sqrt{\left(\frac{\partial R}{\partial x^1} * U_x{}^1\right)^2 + \left(\frac{\partial R}{\partial x^2} * U_x{}^2\right)^2 + \ldots + \left(\frac{\partial R}{\partial x}_n * U_{xn}\right)^2} \quad (8)$$

An error can be classified as systematic or random based on whether it is constant or varies throughout the duration of a single experiment. The maximum uncertainty in Nusselt number R_{th} is calculated as 5.2 % and 5.1 %, respectively.

5. RESULTS AND DISCUSSION

The effect of PPI on the base temperature of the FMFHS at different air velocities is illustrated in **Fig. 8**. An increase in PPI from 5 to 20 leads to a rise in base temperature, as the higher foam density and reduced permeability obstruct air flow and diminish convective heat transfer. All heat sinks record higher temperatures at an air velocity of 2.5 m/s, indicating that the low air velocity is sufficient to produce forced convection. When the velocity increases to 3 m/s, the base temperature of heat sink drops due to greater convective efficiency at higher air movement. At 3.5 m/s, the cooling performance further improves, and the temperature difference between PPI 5 and 10 becomes smaller. In another case, PPI 20 still has the highest temperature because of a higher flow resistance and reduced air penetration. Physically, increasing PPI enhances the solid matrix area and conductive heat transfer; however, under forced convection conditions, the reduction in airflow permeability becomes the dominant factor affecting thermal performance. Accordingly, MFHS with PPI 5 provides the best thermal performance by maintaining an effective balance between heat transfer surface area and airflow passage.

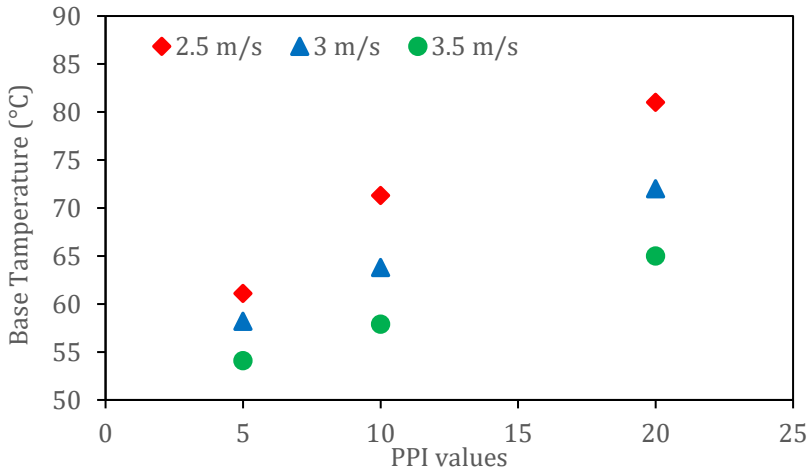

Figure 8. Effect of pore density (PPI) on the base temperature of the MFHS at different air velocities.

The variation of base temperature with air velocity for different pore densities (PPI 5, 10, and 20) of MFHS compared with CHS is shown in **Fig. 9**, As air velocity increases from 2.5 to 3.5 m/s, the base temperature decreases for all configurations due to enhanced convective heat transfer. The 5-PPI foam showed the lowest base temperature, demonstrating superior cooling performance among the tested samples. This demonstrates that pore density is mostly controlled by permeability effects and airflow velocity dominant role in heat removal. Despite the increased surface area in higher PPI configurations, the 10-PPI foam showed reduced performance due to airflow restriction, whereas the 20-PPI sample recorded the highest temperatures because of increased flow resistance. Consequently, the MFHS with 5-PPI provides the most superior thermal performance among the tested due to its larger pores which allow for greater surface area that enable higher airflow penetration and best

effective heat removal. Despite offering enhanced surface area, the 10 PPI foam geometry shows slightly lesser impact because the pore structure facilities air circulation. The 10PPI foam performs slightly weaker since its smaller pores start to restrict airflow despite a higher surface area. The CHS exhibits better performance than 20-PPI because its solid channels allow weaker airflow. However, its total heat transfer area is smaller than that of the metal foams. At PPI 20, the fine pores restrict airflow circulation, causing higher flow resistance and reduced thermal performance.

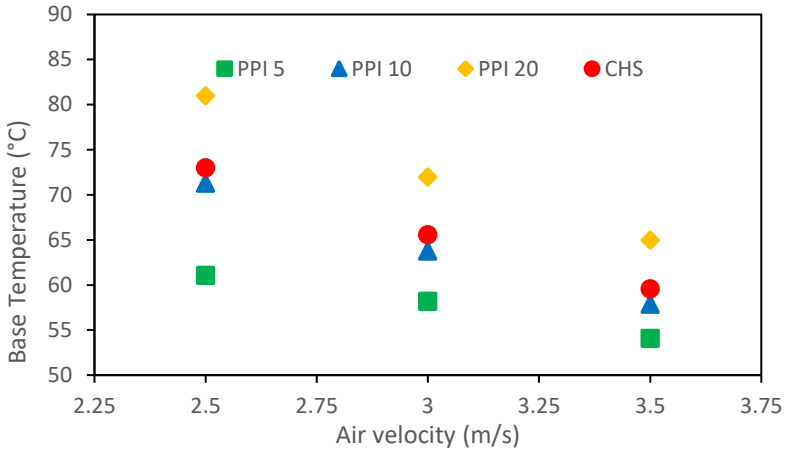

Figure 9. Effect of air velocity on the base temperature for different pore densities (PPI) of the MFHS and CHS.

The variation of the Nusselt number with pore density (PPI 5, 10, and 20) for FMFHS under different air velocities is illustrated in **Fig. 10**, Nusselt number increases with greater air velocity for every pore density, indicating more powerful convective heat transfer. Among all samples, 5-PPI shows the greatest Nusselt number, particularly at 3.5 m/s, the improvement in the Nusselt number achieved 21.6% due to larger pores that enhance air movement and turbulence. This leads to better mixing between the solid and fluid phases, enhancing heat removal from the foam surface. At 10-PPI, the Nusselt number slightly decreases because smaller pores increase flow resistance and limit air penetration. For 20-PPI, the structure restricts airflow significantly, causing poorer convective results in general.

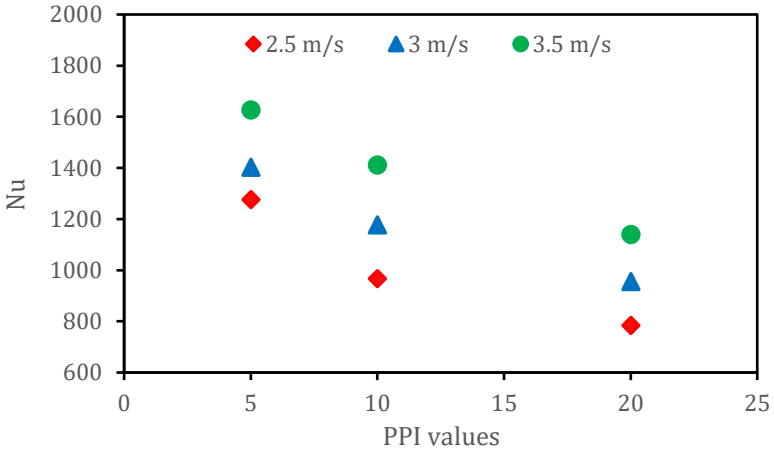

Figure 10. Variation of Nusselt number with pore density (PPI) of the MFHS at different air velocities.

Overall, this figure demonstrates that pore density represents an important parameter in how well heat moves. At higher air velocities, increased Reynolds numbers enhance convective heat transfer. Metal foam with lower pore density therefore showed superior performance, with the 5-PPI heat sink achieving the highest thermal efficiency.

Fig. 11, shows Nusselt number response to metal foam heat sinks in varying air velocities with three pore densities of 5, 10, 20 PPI and a conventional heat sink (CHS). In each case, Nusselt values increase as air speed rises from 2.5 to 3.5 m/s, indicating that faster airflow improves convective cooling. The 5-PPI foam consistently performed the greatest Nusselt number, supporting its superior thermal performance. This outcome stems from the pore size, which facilitates airflow penetration and turbulence, leading to enhanced heat removal. The 10-PPI foam shows moderate performance due to reduced air velocity through smaller pores, while the 20-PPI foam gives lower Nusselt numbers because of airflow restriction and increased flow resistance. While the CHS performs better than the 20-PPI foam, it remains less effective than foams with larger pore sizes. This behavior indicates that forced convection dominates heat transfer at higher velocities. Overall, the 5-PPI structure achieved the most efficient convective heat transfer among the tested designs.

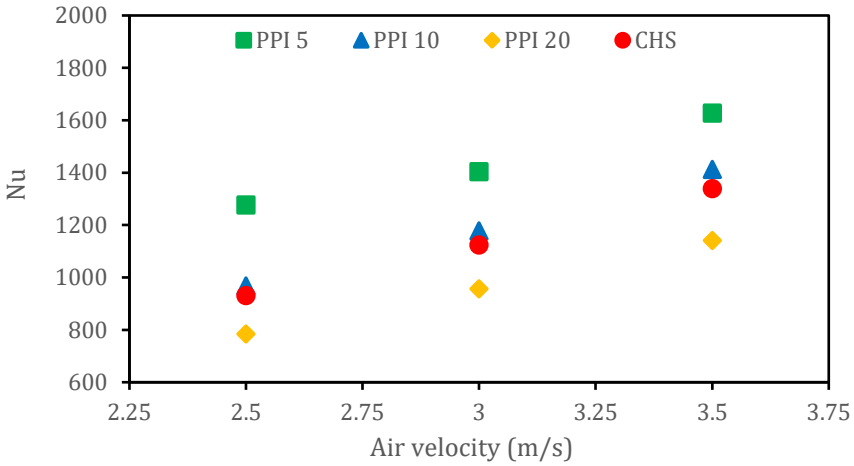

Figure 11. Effect of air velocity on Nusselt number for different pore densities (PPI) of the MFHS and CHS.

As shown in **Fig. 12**, the influence of air velocity on Rth of MFHS with distinct PPI values (5, 10, and 20). The analysis indicates that thermal resistance is significantly decreased with increasing air velocity from 2.5 to 3.5 m/s for all foam types, owing to higher forced convection. The lowest Rth values and a reduction of 16.9% for the PPI 5 heat sink are reported for each of the configurations confirming the stronger performance across the thermal transfer. Because its larger pores facilitate airflow penetration and enhance convective heat removal. The resistance of the PPI 10 sample is slightly higher since smaller pores start to block the passage of air. The highest Rth is caused by its dense structure at PPI 20 due to the high flow restriction and poor air circulation. The reduced temperature difference between the base and outlet at higher flow rates reflects enhanced heat dissipation. Consequently, low-density foams (PPI 5) combined with increased air velocity lead to lower thermal resistance under forced convection.

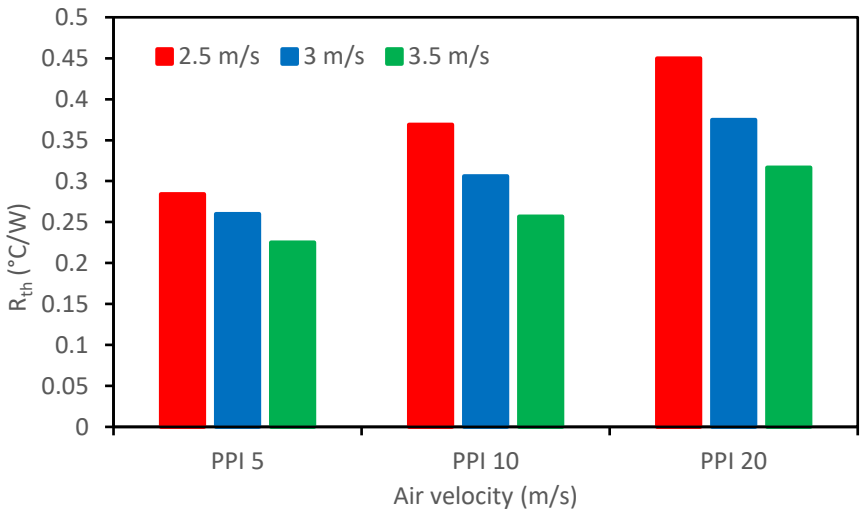

Figure 12. Effect of air velocity on thermal resistance (R_{th}) for different pore densities (PPI) of the MFHS.

Fig. 13 illustrates the impact of air velocity on the Rth for 3 different pore densities (PPI 5, 10, and 20), with MFHS versus CHS. The findings also indicate that for all configurations, the Rth decreases at 2.5–3.5 m/s of air velocity because of the increased forced convection. From a physical standpoint, the reduction in thermal resistance is associated with the enhanced convective heat transfer coefficient and the improved heat exchange between the solid matrix and the airflow as velocity increases. The 5-PPI metal foam, among all tested, had the lowest thermal resistance and therefore displays superior heat removal. This trend is primarily attributed to its high permeability, which facilitates weaker airflow penetration and ensures more uniform heat dissipation across the foam structure.

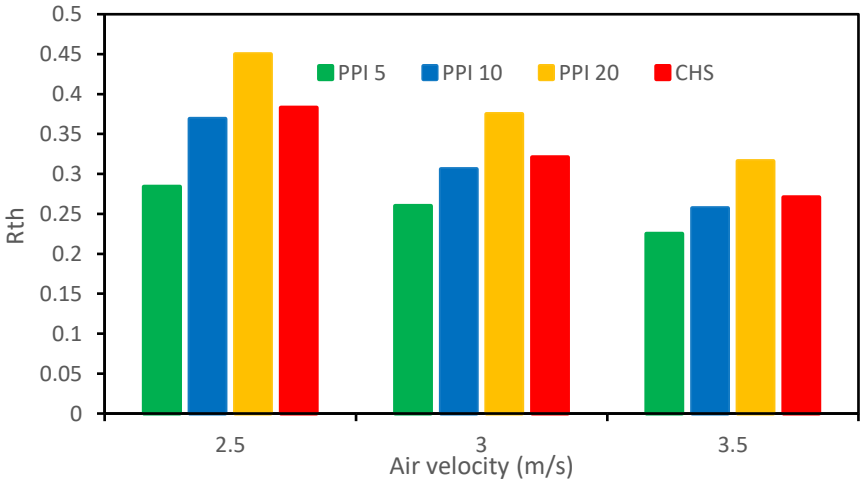

Figure 13. Effect of air velocity on thermal resistance (R_{th}) for different pore densities (PPI) of the MFHS and CHS.

The resistance of the metal foam 10-PPI presents some moderate resistance, while small pores slightly restrict airflow and reduce the cooling rate. The highest Rth value is for the PPI 20 foam, which possesses a highly packed structure that causes a resistance to flow and a reduction in the capacity of convective transport. CHS does better than 20-PPI metal foam, but worse than open-cell foams with low pore densities. In increasing air velocity, the slope

in temperature gradient of the heat sink also diminishes, and the overall thermal resistance is lower. These results confirm that thermal resistance accurately reflects the combined influence of airflow and pore morphology on overall heat sink performance.

6. CONCLUSIONS

The experimental work conducted to evaluate the influence of pore density and air velocity on the thermal performance of FMFHS was specifically designed for high-power CPU cooling. The study was carried out under a constant heat input of 120 W and forced convection conditions, copper foams with different values of 5, 10, and 20 PPI with 90% porosity to determine the most efficient configuration that minimizes thermal resistance and enhances heat dissipation compared with the CHS.

1. The tests demonstrated that reducing the pore density from 20 to 5 PPI leads to a significant enhancement in thermal performance. Among all tested samples, the 5-PPI metal foam consistently achieved the lowest base temperature under all airflow conditions.
2. Thermal resistance analysis confirms that the 5-PPI configuration delivers the most efficient heat transfer performance, owing to its higher permeability, which permits deeper airflow penetration and more effective convective heat removal compared with higher PPI foams.
3. The 10-PPI foam performed at a moderate rate, whereas the 20-PPI foam had the poorest results because its fine pores increased flow resistance and restricted air movement.
4. At an input power of 120 W and an air velocity of 3.5 m/s, the 5-PPI configuration enhanced heat dissipation by 21.6% and reduced thermal resistance by 16.9% compared with the CHS. Highlighting its superior cooling capability.
5. It is therefore recommended to use low-PPI finned copper foam in high-power CPU cooling applications to present a compact design and superior thermal management.

NOMENCLATURE

Symbol	Description	Symbol	Description
A	area of the base heat sink (m^2)	P_0	electric power input (W)
D_h	hydraulic diameter (m)	Q	heat transfer rate from the heated wall (W)
H	height of the heat sink (m)	Re	Reynolds number (-)
h	heat transfer coefficient ($W/m^2.K$)	R_{th}	thermal resistance (°C/W)
I	input current (A)	S	width of the heat sink (m)
K	thermal conductivity (W/m.K)	T	temperature (°C or K)
P	wetted diameter of fin channel (m)	V	input voltage (V)

Acknowledgements

The author expresses gratitude to the entire team of the Mechanical Engineering Department at the College of Engineering, University of Baghdad, for their valuable help and guidance.

Declaration of Competing Interest

The authors declare that they have no known competing financial interests or personal relationships that could have appeared to influence the work reported in this paper.

REFERENCES

Adhikari, R., Wood, D., and Pahlevani, M., 2020. An experimental and numerical study of forced convection heat transfer from rectangular fins at low Reynolds numbers. *International Journal of Heat and Mass Transfer*, 163, P. 120418. https://doi.org/10.1016/j.ijheatmasstransfer.2020.120418.

Ali, H.M., Saieed, A., Pao, W. and Ali, M., 2018. Copper foam/PCMs based heat sinks: an experimental study for electronic cooling systems. *International Journal of Heat and Mass Transfer*, *127*, pp. 381-393.

Ali, R.M.K., and Ghashim, S.L., 2023. Numerical analysis of the heat transfer enhancement by using metal foam. *Case Studies in Thermal Engineering*, 49, P. 103336. https://doi.org/10.1016/j.csite.2023.103336.

Andreozzi, A., Bianco, N., Iasiello, M. and Naso, V., 2017, January. Numerical study of metal foam heat sinks under uniform impinging flow. In *Journal of Physics: Conference Series,* 796(1), P. 012002. https://doi.org/10.1088/1742-6596/796/1/012002.

Bayomy, A.M., Saghir, M.Z. and Yousefi, T., 2016. Electronic cooling using water flow in aluminum metal foam heat sink: Experimental and numerical approach. *International Journal of Thermal Sciences*, *109*, pp. 182-200. https://doi.org/10.1016/j.ijthermalsci.2016.06.007.

Bianco, N., Iasiello, M., Mauro, G.M. and Pagano, L., 2021. Multi-objective optimization of finned metal foam heat sinks: Tradeoff between heat transfer and pressure drop. *Applied Thermal Engineering*, *182*, P. 116058. https://doi.org/10.1016/j.applthermaleng.2020.116058

De Schampheleire, S., De Jaeger, P., De Kerpel, K., Ameel, B., Huisseune, H. and De Paepe, M., 2016. How to study thermal applications of open-cell metal foam: Experiments and computational fluid dynamics. *Materials*, *9*(2), P. 94. https://doi.org/10.3390/ma9020094.

Feng, S.S., Kuang, J.J., Lu, T.J. and Ichimiya, K., 2015. Heat transfer and pressure drop characteristics of finned metal foam heat sinks under uniform impinging flow. *Journal of Electronic Packaging*, *137*(2), P. 021014.https://doi.org/10.1115/1.4029722.

Güler, N., Bayer, Ö., and Solmaz, İ., 2024. Experimental and numerical investigation on fluid flow and heat transfer behaviour of foam cladded pin fin heat sink. *Applied Thermal Engineering*, 256, P. 124184. https://doi.org/10.1016/j.applthermaleng.2024.124184.

Haghighi, S.S., Goshayeshi, H.R., and Zahmatkesh, I., 2024. Experimental investigation of forced convection heat transfer for different models of PPFHS heatsinks with different fin-pin spacing. *Heliyon*, 10(1)

Hao, G.H., and Zhang, Y.P., 2019. Thermal Performance Simulation of the Metal Foam Heat Sink. In Solid State Phenomena, pp. 208-213.

Heydari, A., Mesgarpour, M., and Gharib, M.R., 2020. Experimental and Numerical Study of Heat Transfer and Tensile Strength of Engineered Porous Fins to Estimate the Best Porosity. *Jordan Journal of Mechanical & Industrial Engineering*, 14(3), pp. 339 - 348.

Hoi, S.M., Teh, A.L., Ooi, E.H., Chew, I.M.L., and Foo, J.J., 2019. Plate-fin heat sink forced convective heat transfer augmentation with a fractal insert. *International Journal of Thermal Sciences*, 142, pp. 392-406. https://doi.org/10.1016/j.ijthermalsci.2019.04.035.

Holman, J.P., 2012. *Experimental methods for engineers*. New York: McGraw-Hill series in mechanical engineering.

Kanate, V., Pardeshi, A., Charde, F., Kolase, K., Bhise, A. and Kothmire, P., 2022, December. Numerical Investigation on Performance of CPU Heat Sinks. In *Conference on Fluid Mechanics and Fluid Power*, pp. 361-372. Singapore: Springer Nature Singapore.

Kim, S.Y., Paek, J.W. and Kang, B.H., 2003. Thermal performance of aluminum-foam heat sinks by forced air cooling. *IEEE Transactions on components and packaging technologies*, *26*(1), pp. 262-267.

Li, Y., Gong, L., Xu, M., and Joshi, Y., 2020. Hydraulic and thermal performances of metal foam and pin fin hybrid heat sink. *Applied Thermal Engineering*, 166, P. 114665. https://doi.org/10.1016/j.applthermaleng.2019.114665.

Li, Y., Gong, L., Xu, M., and Joshi, Y., 2021. Thermal performance of metal foam heat sink with pin fins for nonuniform heat flux electronics cooling. *Journal of Electronic Packaging*, 143(1), P. 011006. https://doi.org/10.1115/1.4046756.

Liaw, K.L., Rosle, A.F.H.B., Hendarti, R. and Kurnia, J.C., 2022, December. Thermal Performance Evaluation of Heat Sink with Pin Fin, Metal Foam and Dielectric Coolant. In *International Conference on Renewable Energy and E-mobility*, pp. 35-49. Singapore: Springer Nature Singapore.

Mangate, L., Ghuge, S., Khairnar, A., Dixit, S., Kale, A., Hujare, G., Gholap, S., and Sawant, G., 2025. Investigating the Effect of Heat Sink Material on Processor Thermal Management. I*n 2025 5th International Conference on Innovative Research in Applied Science, Engineering and Technology (IRASET)*, pp. 1-8. *IEEE*.

Mirshekar, A., Goodarzi, M.R., Mohebbi-Kalhori, D., and Mayam, M.H.S., 2023. Experimental study of heat transfer enhancement using metal foam partially filled with phase change material in a heat sink. *Journal of Energy Storage*, 60, P. 106496. https://doi.org/10.1016/j.est.2022.106496.

Moayad, N.A., and Sarsam, W.S., 2025. Theoretical and Experimental Investigation of an Acetone-Filled Pulsating Heat Pipe Heat Exchanger for Waste Heat Recovery. *Journal of Engineering*, 31(9), pp. 191-207. https://doi.org/10.31026/j.eng.2025.09.12.

Mokhiamar, O., Masara, D.O., and El Gamal, H., 2022. Performance Enhancement of Multi-Modal Piezoelectric Energy Harvesting Through Parameter Optimization. *Jordan Journal of Mechanical & Industrial Engineering*, 16(5).

Nawaz, K., Bock, J., Dai, Z., and Jacobi, A.M., 2010. Experimental studies to evaluate the use of metal foams in highly compact air-cooling heat exchangers. *International Refrigeration and Air Conditioning Conference.* Paper 1150. http://docs.lib.purdue.edu/iracc/1150

Nima, M.A., and Hajeej, A.H., 2016. Experimental investigation of convection heat transfer enhancement in horizontal channel provided with metal foam blocks. *Journal of Engineering*, 22(5), pp. 144-161. https://doi.org/10.31026/j.eng.2016.05.10.

Pires-Fonseca, W.D., and Carrasco-Altemani, C.A., 2024. Experimental and numerical investigation of flat plate fins and inline strip fins heat sinks. *Revista Facultad de Ingeniería Universidad de Antioquia*, 110, pp. 86-98.

Qiu, T., Wen, D., Hong, W., and Liu, Y., 2020. Heat transfer performance of a porous copper micro-channel heat sink. *Journal of Thermal Analysis and Calorimetry*, 139(2), pp. 1453-1462.

Radmanesh, A., Dukhan, N., Liang, M., and Engels, J., 2023. Optimization of Metal Foam Heat Sinks for Electronic Air Cooling: Part I: Porosity. *In 2023 22nd IEEE Intersociety Conference on Thermal and Thermomechanical Phenomena in Electronic Systems (ITherm),* pp. 1-5. *IEEE*.

Rashid, F.L., Talib, S.M., and Hussein, A.K., 2022. An Experimental Investigation of Double Pipe Heat Exchanger Performance and Exergy Analysis Using Air Bubble Injection Technique. *Jordan Journal of Mechanical & Industrial Engineering*, 16(2), pp. 195 - 204.

Shadlaghani, A., Tavakoli, M., Farzaneh, M., and Salimpour, M., 2016. Optimization of triangular fins with/without longitudinal perforate for thermal performance enhancement. *Journal of Mechanical Science and Technology*, 30(4), pp. 1903-1910.

Singh, N.R., Onkar, S., and Ramkumar, J., 2021. Thermo-hydraulic performance of square micro pin fins under forced convection. *International Journal of Heat and Technology,* 39(1), pp. 170-178. https://doi.org/10.18280/ijht.390118

Theeb, A.H.F., and Hussain, I.Y., 2024. A Review of the Thermal Phase Change Materials (PCM) and Metal Foams for Electronic Chips Cooling. *Al-Iraqia Journal for Scientific Engineering Research*, 3(4), pp. 1-13.

Uglah, A.M., and Jubear, A.J., 2020. Numerical thermal performance of free convection in metal foam heat sinks with fin edges. *University of Thi-Qar Journal for Engineering Sciences*, 11(1), pp. 19-30. https://doi.org/10.31663/tqujes.11.1.375(2020).

Wang, Y., Ma, X., Ouyang, Z., and Liang, S., 2025. Comprehensive analysis of forced convection heat transfer enhanced by metal foam with pore density gradient structure. *Solar Energy Materials and Solar Cells*, 285, P. 113549.

Welsford, C., Thanapathy, P., Bayomy, A.M., and Saghir, M.Z., 2018. Thermal Performance in High Porosity Open-Cell Aluminum Foams. *In ICTEA: International Conference on Thermal Engineering,* pp. 1-3.

Xiong, J., Sun, J., Chen, Y., and Nie, Z., 2024. Study on the flow and heat transfer characteristics inside high-porosity open-cell copper foams: Experimental and numerical explorations. *International Journal of Heat and Fluid Flow*, 109, P. 109499. https://doi.org/10.1016/j.ijheatfluidflow.2024.109499.

Younus, S.M., and Abedalh, A.S., 2025. Enhancement the performance of the heat sink by using metal foam partially immersed in phase change materials for different porosities. *Energy Technology*, P. 2500774.

Yudanto, F.D., Inderanata, R.N., Johan, A.B., and Setuju, S., 2023. Numerical study optimation design of CPU cooling system analysis using CFD method. *Applied Engineering and Technology*, 2(3), pp. 241-253.

Zografos, A.I., Martin, W.A., and Sunderland, J.E., 1987. Equations of properties as a function of temperature for seven fluids. *Computer Methods in Applied Mechanics and Engineering*, 61(2), pp. 177-187.

أداء تبديد الحرارة لوحدات المعالجة المركزية ذات القدرة العالية باستخدام مشتتات حرارية من رغوة النحاس المزودة بالزعانف

سهى شذر اسماعيل ، وائل سامي سرسم *

قسم الهندسة الميكانيكية، كلية الهندسة، جامعة بغداد، بغداد، العراق

الخلاصة

يعتبر التخلّص الفعّال من الحرارة تحديًا رئيسيًا في أنظمة وحدات المعالجة المركزية (CPU) عالية القدرة، إذ إن ارتفاع درجات حرارة السطح قد يؤدي إلى تراجع الأداء وانخفاض الاعتمادية. يتناول هذا العمل دراسة تجريبية لأداء تبديد الحرارة لمشتت حراري مصنوع من رغوة معدنية من النحاس ذو زعانف، صُنِع بثلاث قيم مختلفة للكثافة المسامية 5,10,20 PPI مسام لكل إنش مع الحفاظ على مسامية مقدارها 90%. وقد جرت مقارنة هذه النماذج بمشتت حراري تقليدي ذي زعانف صفائحية من الألمنيوم. أُجريت الاختبارات تحت ظروف الحمل الحراري القسري باستخدام سرعات هواء مقدارها (2.5 ,3.0 ,3.5) م/ث، وبدرجة حرارة الهواء المحيط تبلغ 27°م، مع حمل حراري ثابت مقداره 120 واط. وأظهرت النتائج وجود تأثير واضح لحجم المسام في سلوك التبريد؛ إذ حققت الرغوة المعدنية ذات الكثافة المسامية 5 PPI أعلى أداء حراري، نتيجة امتلاكها فتحاتٍ أكبر تسمح بنفاذية أعلى للهواء وتحسّن انتقال الحرارة بالحمل القسري .في المقابل، سجّلت الرغوة ذات 20 PPI معدلات أقل في إزاحة الحرارة. وقد حقق تصميم 5 PPI زيادة عدد نسلت بنسبة 21.6% في معدل تبديد الحرارة، وانخفاضًا في المقاومة الحرارية بنسبة 16.9%، عند السرعة 3.5 م/ث والحمل حراري يبلغ 120 واط، مقارنة بالمشتت الحراري التقليد .أما رغوة النحاس ذات 10 PPI فقد أظهرت أداءً متوسطًا يقع بين نموذج 5 PPI والنموذج المرجعي وتؤكد هذه النتائج أن استخدام الرغوات النحاسية منخفضة الكثافة المسامية ضمن هندسة مزوّدة بزعانف يؤدي إلى تعزيز ملحوظ في كفاءة التبريد للمكونات الإلكترونية عالية القدرة. وبناءً على ذلك، يُوصى باعتماد مشتتات حرارية مصنوعة من رغوة النحاس منخفضة الـ PPI في أنظمة تبريد وحدات المعالجة المركزية عالية القدرة، خاصةً في التطبيقات التي تتطلّب حجمًا مدمجًا وكفاءة حرارية مرتفعة.

الكلمات المفتاحية: مشعات حرارية من رغوة معدنية ذات زعانف، رغوة معدنية، كثافة المسام، الحمل الحراري القسري، المقاومة الحرارية.